Silicone Oil Damping for Quasi-static Micro Scanners with Electrostatic Staggered Vertical Comb Drives

Richard Schroedter[*,]. Jan Grahmann[*]. Klaus Janschek[***]**

[*] *Fraunhofer Institute for Photonic Microsystems, Active Microscanner Systems, Maria-Reiche-Str.2, 01109 Dresden, Germany (Tel: +49 351 8823-196; e-mail: jan.grahmann@ipms.fraunhofer.de).*
[**] *Automation and Control Institute (ACIN), Faculty of Electrical Engineering and Information Technology, TU Wien, Gußhausstraße 27-29, 1040 Wien, Austria (e-mail: schroedter@acin.tuwien.ac.at).*
[***] *Institute of Automation, Faculty of Electrical and Computer Engineering, Technische Universität Dresden, 01062 Dresden, Germany (Tel: +49 351 463-34025; e-mail: klaus.janschek@tu-dresden.de)*

Many applications like image projection, distance sensors or spectroscopy require high speed quasi-static operating scanners with the size of several millimeters for the laser beam guidance. Quasi-static micro scanners with electrostatic staggered vertical comb drives of sizes up to 5 mm achieve remarkable mechanical deflections of ±8 degree and eigenfrequencies of several hundred Hertz. Closed-loop control of the scanner position highly reduces parasitic eigenfrequency oscillation when driving an arbitrary trajectory like triangle or saw tooth, but requires position feedback and high performant drive electronics for real-time control. In this contribution we investigate silicone oil to attenuate undesired oscillations by passive mechanic damping. We present experimental results with different viscosity and determine the resulting system parameters such as damping coefficient, eigenfrequency and permittivity, supported by transient simulations. While the permittivity, refractive index and damping increase significantly, the deceasing eigenfrequency results in slower admissible trajectories. The overall performance is assessed and compared to the active damping approach using closed-loop control of the micro scanner operating in air. Finally, a potential packaging technology is presented.

Keywords: laser beam guidance, quasi-static micro scanner, electrostatic staggered vertical comb drive, silicone oil, viscous passive damping, permittivity, close-loop trajectory control

1. INTRODUCTION

Quasi-static micro scanners are broadly applied for mobile imaging and sensing purposes, as in autonomous driving vehicles for light deflection and ranging sensors (LiDAR), e.g. Yoo et al. (2018), Milanović et al. (2017), Park et al. (2018) and Kaupmann et al. (2018), micro beamer like head-up displays, e.g. Chao et al. (2011) and Yalcinkaya et al. (2006), or miniaturized spectroscopes in combination with external cavity quantum cascade lasers, e.g. Jiménez et al. (2018). As proved by Schroedter et al. (2017) micro scanners with electrostatic staggered vertical comb drives fabricated with CMOS compatible processes achieve remarkable mechanical deflections of ±8° at resonance frequencies of several 100 Hz with mirror sizes up to 5 mm. Furthermore, the technology permits a two-dimensional scan in combination with an inner resonant axis. While the resonantly driven scanners benefit from high quality factors, quasi-static scanners suffer from very low damping of the system revealing difficulties in fast and precise beam positioning, because the system's resonance appears while tracking the desired trajectory, cf. Schroedter et al. (2017). An efficient but costly method is trajectory tracking with closed-loop control using on-chip piezoresistive position sensors, e.g. Grahmann et al. (2016), or external sensor, e.g. Baumgart et al. (2015). The highly nonlinear electrostatic comb drive demands nonlinear control schemes like flatness-based control, investigated in Schroedter (2018), and voltages up to 200 V powered by real-time electronic with sampling rates at least ten times higher than the micro scanner eigenfrequency. Nevertheless, quasi-static scanners are designed to achieve linear trajectories (triangular or saw tooth shape) and fast step response times. Passive damping methods for electrostatic comb drives can overcome the disadvantage of complex control strategies that increase the cost of mass production. Here, impedance feedback is limited due to overdamping of the large displacement current through the drive capacitance while the maximum damping increases only by factor two as revealed in Schroedter et al. (2014). This contribution investigates silicone oil as an alternative passive damping strategy for quasi-static micro scanners and analyses the change in performance including inertia, permittivity and refractive index. In addition to the experiments published by Milanović et al. (2016) showing the principle feasibility of oil damping with quasi-static electrostatic micro scanners, this research focuses on the identification of system parameters using an on-chip piezoresistive position sensor and assesses the performance supported by numerical simulations. Finally, the bandwidths for triangular, saw tooth and step trajectories are given and an optimally damped scanner with silicone oil is discussed further.

Post-print version of the article: R. Schroedter, J. Grahmann, K. Janschek, "Silicone Oil Damping for Quasi-static Micro Scanners with Electrostatic Staggered Vertical Comb Drives", *8th IFAC Symposium on Mechatronic Systems*, vol. 52, issue 15, pp. 37-42, 2019. DOI: 10.1016/j.ifacol.2019.11.646

For further information contact: schroedter@acin.tuwien.ac.at, https://orcid.org/0000-0003-3259-4571

The paper is structured as follows: Section 2 introduces the employed micro scanner with electrostatic staggered vertical comb drive, comprising the system modeling in section 2.1 and trajectory results in air in section 2.2. Section 3 presents the silicone oil experiments showing the experimental results in section 3.1, the impulse responses in section 3.2, the trajectory results in oil in section 3.3 as well as simulation results in section 3.4 for comparison. The system is analyzed in section 4 including the damping effect in section 4.1, the permittivity increases in section 4.2, the refraction index in section 4.3 and the eigenfrequency in section 4.4. The overall performance is discussed in section 5. Section 6 gives a potential bubble-free packaging option. Finally, the contribution is summarized in section 7 appending further research goals.

2. MICRO SCANNER WITH ELECTROSTATIC STAGGERED VERTICAL COMB DRIVE

The single crystalline silicone quasi-static micro scanner is powered by an electrostatic staggered vertical comb drive, configured as Fig. 1 shows.

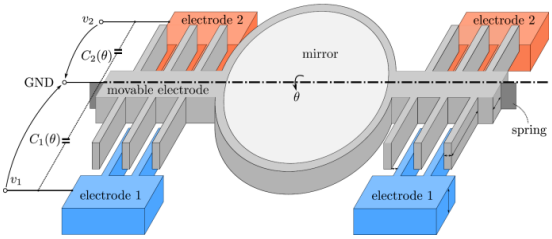

Fig. 1: Schematic of micro scanner with electrostatic staggered vertical comb drive, from Schroedter et al. (2017)

The outer combs (electrodes 1 and 2) are staggered vertically about the substrate height of 75 µm by stamps of a supplement top wafer, which is bonded onto the device wafer, as Jung et al. (2012) describes. This enables a static mechanical deflection up to ±9° at 202 V, resulting in optical field of view of 36°. The comb drive consists of 492 fingers with a pitch of 5 µm and a length of 245 µm. The 2×3 mm^2 large mirror is aluminum coated featuring more than 85 % reflectivity above 400 nm wavelengths. The progressive torsion spring stiffens quadratically up to 30 % at 9°. The first nominal tilt mode is at $f_0 = 560$ Hz, where the following modes like the piston mode at 3 kHz and the translation mode in finger direction near 5 kHz are much higher. The pull-in stability is optimized at 220 V and the shock resistance is designed to withstand 2500 g. The micro scanner easily withstands the automotive LV 124 vibration profile D (LV124, Volkswagen VW 80000, 2013-06, February 2013) corresponding to hang-on-parts without any damage. Further investigations on the trajectory accuracy under external vibration are in progress.
The micro mirror is equipped with a polycrystalline piezoresistive sensor for position feedback as described in Grahmann et al. (2016). This allows feedback control of the mirror dynamics and verification of system performance using silicone oil in comparison to the experiments performed in Milanović et al. (2016).

2.1. System modeling

The mirror system is modeled with (1), where J is the torque inertia, b is the linear viscous damping, $\tau_s(\theta) = \int_0^\theta k(\theta')\,\mathrm{d}\theta'$ is the progressive spring torque with $k(\theta) = k_0 + k_2\theta^2$, $C'_{1,2}(\theta) := \mathrm{d}C_{1,2}(\theta)/\mathrm{d}\theta$ are the drive capacitance derivatives and $v_{1,2}$ are the drive voltages.

$$J\ddot{\theta} + b\dot{\theta} + \tau_s(\theta) = \frac{1}{2}C'_1(\theta)\cdot v_1^2 + \frac{1}{2}C'_2(\theta)\cdot v_2^2 \qquad (1)$$

The torque inertia $J = 0.5$ kg µm^2 (in air) and the nonlinearity $k_2 = 64.5$ µNm/rad of the spring stiffness result from an ANSYS simulation. The linear stiffness $k_0 = J\omega_0^2 = 6.2$ µNm and the damping $b = 2DJ\omega_0 = 1.7 \cdot 10^{-11}$ Nms (in air) are evaluated by fitting the decaying sinusoidal oscillation (2) to the experimental data of the impulse response.

$$\theta(t) = \hat{\theta}\cdot e^{-2D\omega_0 t}\cdot\cos\left(\sqrt{1-D^2}\omega_0 t\right) \qquad (2)$$

The capacitance derivatives shown in Fig. 3 are determined from the static voltage-deflection curve measurements given in Fig. 2 using the relation $C'_{1,2}(\theta) = 2\,\tau_s(\theta)/v_{1,2}^2$ for each comb electrode individually. To handle the singularity for zero voltage, the capacitance derivative is extrapolated exponentially; cf. Schroedter et al. (2014).

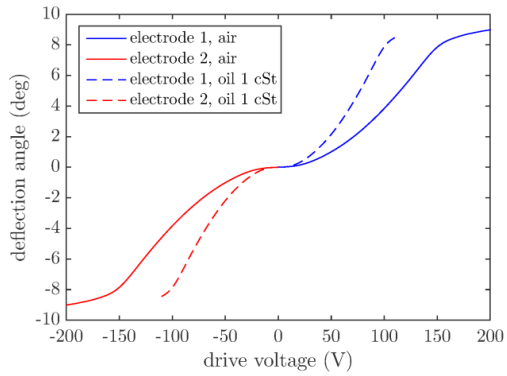

Fig. 2: Measured static voltage-deflection curve of electrodes 1 (blue) and 2 (red): air (line) and oil with 1 cSt (dashed line)

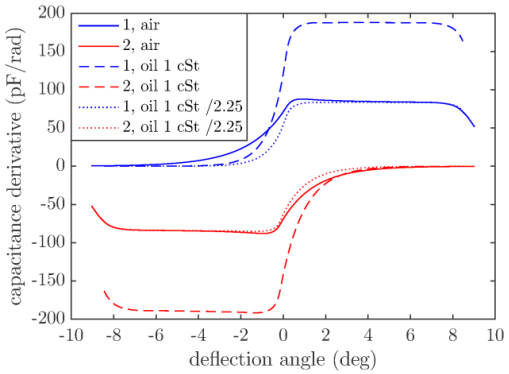

Fig. 3: Capacitance derivatives of electrodes 1 (blue) and 2 (red): air (line), oil 1 cSt (dashed), curve of oil 1 cSt scaled by factor 2.25. The curves are extrapolated exponentially for not immersed combs.

Post-print version of the article: R. Schroedter, J. Grahmann, K. Janschek, "Silicone Oil Damping for Quasi-static Micro Scanners with Electrostatic Staggered Vertical Comb Drives", *8th IFAC Symposium on Mechatronic Systems*, vol. 52, issue 15, pp. 37-42, 2019. DOI: 10.1016/j.ifacol.2019.11.646

For further information contact: schroedter@acin.tuwien.ac.at, https://orcid.org/0000-0003-3259-4571

The piezoresistive sensor (WHEATSTONE bridge) is calibrated when measuring the static deflection using a specified electronic with a gain of 35. This reveals a mainly linear sensor characteristic with a sensitivity of 7.8°/V and a standard deviation (equivalent to root mean square error (RSME)) of about 6.9 mdeg (millidegree) over ±8.3° and a signal-to-noise ratio of 68 dB as shown in Fig. 4. The sensor characteristic has a small nonlinearity of ±3.4 %. Therefore, finally a 30th order polynomial fit is applied as sensor curve.

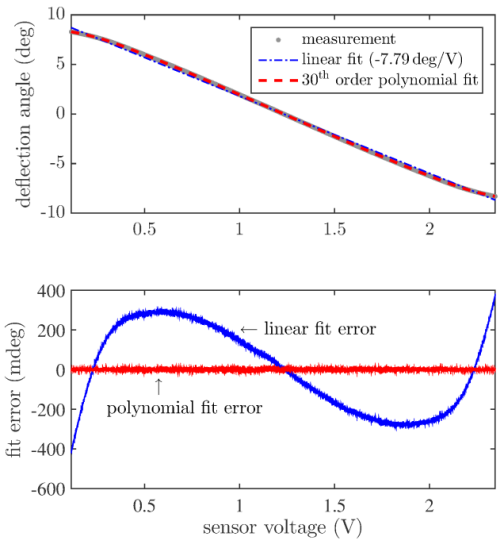

Fig. 4: Measured piezoresistive sensor characteristic: linear fit with RSME = 213 mdeg and 30th order polynomial fit with $\sigma = 6.9$ mdeg

2.2. Trajectory results

The micro scanner can be driven any trajectory considering a dynamic below the system's eigenfrequency f_0, because of its unidirectional actuation. To cope with the low system damping in air, an open loop flatness-based feed forward control is applied as described in Schroedter et al. (2017), which inverts the system dynamic given by (1). Nevertheless, small model inaccuracies lead to residual oscillation as shown in Fig 5 and 6 (open loop). The model is in particular imprecise at zero deflection because of the singularity near zero deflection explained in section 2.1. Furthermore, asymmetric torque injection of the staggered vertical comb drive pulls the mirror slightly into parasitic motions in direction of the comb fingers and the piston mode. In closed loop mode using flatness-based feed forward control with output stabilization, as depicted in Schroedter (2018), the main oscillation is highly damped as shown in Fig 5 and 6 (closed loop). The ringing decay time of the error is about 15 ms. Currently, a major restriction of the control gain and the observer poles is a parasitic coupling of the high voltage drive current into the low piezoresistive voltage sensor signal, that leads to an internal noise feedback in the control loop. Here, a capacitive coupling between the wires on the micro mirror chip is assumed.

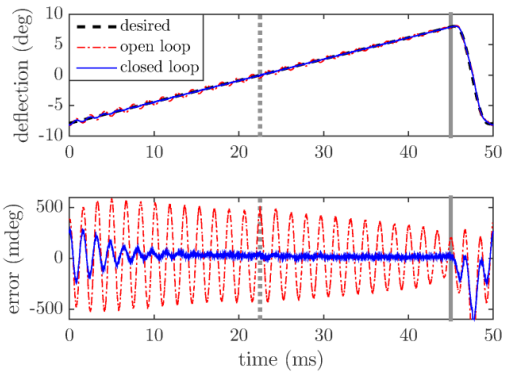

Fig. 5: Experimental result **in air** of 20 Hz saw tooth trajectory (±8°, 90 % linear time) measured with piezoresistive sensor: result (upper) and error towards desired (lower)

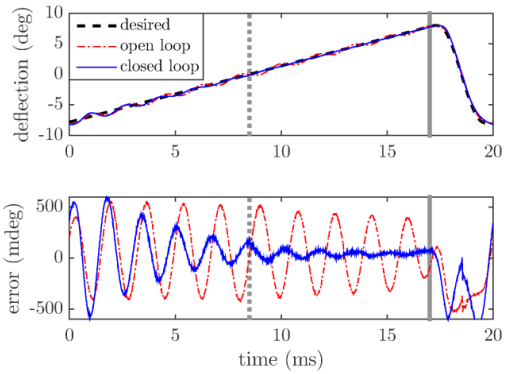

Fig. 6: Experimental result **in air** of 50 Hz saw tooth trajectory (±8°, 80 % linear time) measured with piezoresistive sensor: result (upper) and error towards desired (lower)

3. SILICONE OIL EXPERIMENTS

The mirror is glued on a printed circuit board (PCB) and connected via wire bonds. A plastic frame and a glas cover build the cavity for the silicone oil. In the experiments, the silicone oil is injected from the backside hole in the PCB under the mirror and the cavity is closed by a tape. An air bubble remains, but all electrostatic combs are fully filled with oil as Fig. 7 (right) shows. Fig. 7 (left) shows the experimental setup inlcuding the scanner driver electronics.

3.1. Experimental setup

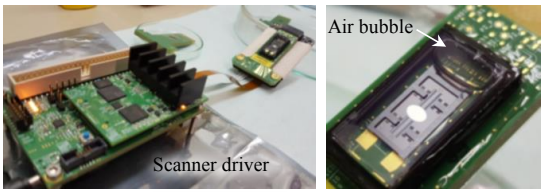

Fig. 7: Photograph of experimental setup with electronics (left) and micro scanner cavity filled with silicone oil showing a remaining air bubble (right)

Post-print version of the article: R. Schroedter, J. Grahmann, K. Janschek, "Silicone Oil Damping for Quasi-static Micro Scanners with Electrostatic Staggered Vertical Comb Drives", *8th IFAC Symposium on Mechatronic Systems*, vol. 52, issue 15, pp. 37-42, 2019. DOI: 10.1016/j.ifacol.2019.11.646

For further information contact: schroedter@acin.tuwien.ac.at, https://orcid.org/0000-0003-3259-4571

After characterization in air as described in section 2, silicone oil with a viscosity of 1 centi Stokes (cSt) and in a second later experiment of 3 cSt is applied. The silicone oil parameters given by manufacturer are summarized in Tab. 1. All experiments are performed with the same micro scanner.

Tab. 1: Silicone oil parameter at 25°C given by manufacturer (ELBESIL QUAX GmbH) compared to air

Medium	Kinematic viscosity in centi Stokes (cSt) or mm^2/s	Refractive index n	Density in g/cm^3
Air	-	1	0.001
Silicone oil 1 cSt	1	1.38	0.816
Silicone oil 3 cSt	3	1.397	0.90

3.2. Impulse responses

The impulse responses are acquired with the piezoresistive sensor by applying an impulse voltage as given in Tab. 2 within 940 µs. The experimental results are shown in Fig. 8. The eigenfrequency and damping, respective quality factor, are evaluated by fitting the measurement data to (2). The regression reveals a high agreement with the coefficients of determination R^2: 98.5 (air), 99.9 (silicone oil 1 cSt) and 98.3 (silicone oil 3 cSt).

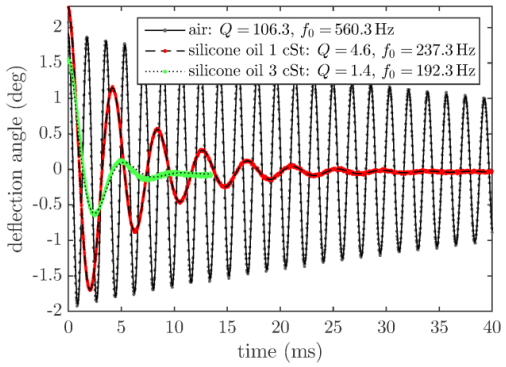

Fig. 8: Impulse responses in different viscous media as dots and decay fit curves as lines: air (gray, line), silicone oil 1 cSt (red, dashed line) and silicone oil 3 cSt (green, dotted line)

Tab. 2: Experimental results of 940 µs impulse responses

Medium	Impulse voltage in V	Eigen-frequency f_0 in Hz	Quality factor Q	Equiv. torque inertia J in $kg\mu m^2$
Air	7	560.3	106.3	0.5*
Silicone oil 1 cSt	50	237.3	4.6	2.79**
Silicone oil 3 cSt	90	192.3	1.4	4.24**

*ANSYS result, **experimental result using (3)

3.3. Trajectory results

The trajectory results with silicone oil 1 cSt in Fig. 9 and 10 prove well the passive damping effect of silicone oil, compared to air (cf. Fig. 5 and 6). The trajectory error reveals an offset of 100 mdeg when changing between electrode 1 and 2. This may be caused by a calibration error due to insufficient slow calibration performed with a 0.1 Hz sine voltage acquiring the static deflection characteristic (cf. Fig. 2).

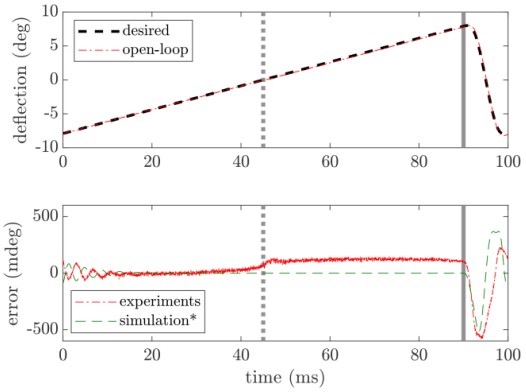

Fig. 9: Experimental result **in silicone oil** 1 cSt of 10 Hz saw tooth trajectory (+-8°, 90 % linear time) measured with piezoresistive sensor: result (upper) and error towards desired (lower), *numerical simulation result

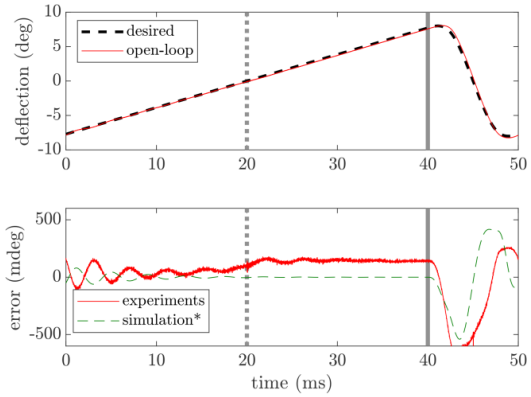

Fig. 10: Experimental result **in silicone oil** (1 cSt) of 20 Hz saw tooth trajectory (+-8°, 80 % linear time) measured with piezoresistive sensor: result (upper) and error towards desired (lower), *numerical simulation result

3.4. Simulation study

The mirror dynamic was simulated in MATLAB/SIMULINK with concentrated parameters. The resulting error is shown as green dashed curve in Fig. 9 and Fig. 10. To reveal the mirror dynamic of the experiment the original mirror inertia without silicone oil was applied in the flatness-based feed forward model. This leads to a small eigenfrequency oscillation at the beginning of the period showing a high agreement in the error amplitude between measurement and simulation. When applying the corrected mirror inertia as given in Tab. 2, the simulation error disappears due to the high damping.

Post-print version of the article: R. Schroedter, J. Grahmann, K. Janschek, "Silicone Oil Damping for Quasi-static Micro Scanners with Electrostatic Staggered Vertical Comb Drives", *8th IFAC Symposium on Mechatronic Systems*, vol. 52, issue 15, pp. 37-42, 2019. DOI: 10.1016/j.ifacol.2019.11.646

For further information contact: schroedter@acin.tuwien.ac.at, https://orcid.org/0000-0003-3259-4571

4. SYSTEM ANALYSIS

In the following, the experimental results are evaluated in a general system analysis comparing air with silicone oil.

4.1 Damping effect

Eigenfrequency and damping are evaluated by fitting (2) to the experimental impulse response data, as given in Tab. 2, applying the relations for quality factor $Q = 1/(2D)$ and frequency $\omega_0 = 2\pi f_0$. Here, the damping rises by factor 23 with 1 cSt oil and by factor 76 with 3 cSt oil.

4.2 Permittivity increase

The silicone oil leads to an increase in permittivity compared to air. This results from the static deflection curve shown in Fig. 2. The static deflection curve in oil corresponds to those in air by multiplying factor 1.5 in x-axis (voltage), which equals to an increase in permittivity by factor $\varepsilon_r = 2.25$. This scaling is proved by the high agreement of the curves in air (line) compared to silicone oil 1 cSt divided by 2.25 (dotted line) in Fig. 3.

4.3. Refraction index

The silicone oil has the positive effect of increasing the refractive index, as given in Tab. 1. The beam path is sketched in Fig. 11. Consequently, silicone oil increases the optical beam output angle about 38 % with 1 cSt and 40 % with 3 cSt respectively.

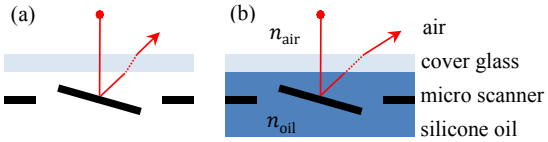

Fig. 11: Beam path with micro scanner (a) in air, (b) in silicone oil

4.4. System eigenfrequency

A negative effect of the gain in damping is the loss in eigenfrequency due to the increase in total torque inertia caused by the moving silicone oil. Since the systems stiffness remains in the spring, the torque inertia and damping coefficient for silicone oil can be obtained by (3):

$$J_{\text{oil}} = \frac{k_{0,\text{air}}}{4\pi^2 f_{0,\text{oil}}^2}, \qquad b_{\text{oil}} = \frac{k_{0,\text{air}}}{2\pi f_{0,\text{oil}} \cdot Q_{\text{oil}}}. \tag{3}$$

Considering a homogeneous silicone oil film on the mirror surface, causing the increase in moved mass, the height of this oil film would be 1.33 mm on each side for silicone oil 1 cSt and 1.41 mm for silicone oil 3 cSt respectively.
Consequently, the eigenfrequency decreases by factor 2.4 with silicone oil 1 cSt and by factor 2.9 with silicone oil 3 cSt respectively. This leads to a significant loss in mirror dynamics compared to air. The maximum trajectory repetition rates for jerk-limited trajectories within the voltage limits are derived in Schroedter (2018) for triangle f_∇ and sawooth $f_\vartriangle$ shape according the eigenfrequency f_0, resulting in:

$$f_\nabla = f_0 \cdot \frac{\pi}{2}\frac{\sqrt{3}}{6}\sqrt{4 - 2\kappa_{\text{lin}} - 2\kappa_{\text{lin}}^2}\,, \tag{4a}$$

$$f_\vartriangle = f_0 \cdot \frac{\pi}{2}\frac{1-\kappa_{\text{lin}}}{\sqrt{3}}\sqrt{3\kappa_{\text{lin}} + (1-\kappa_{\text{lin}})^{\frac{3}{2}}}\,. \tag{4b}$$

In (4) $\kappa_{\text{lin}} = t_{\text{lin}}/T = 0 \ldots 1$ denotes the relation of linear time t_{lin} towards the period time $T = 1/f$.
Furthermore, for the step response the shortest step time is:

$$t_S = \frac{\sqrt{2}}{\pi}\frac{1}{f_0}. \tag{5}$$

The decrease in trajectory repetition rate and step time is given in Tab. 3, revealing the loss in dynamics by passive damping with silicone oil.

Tab. 3: Maximum trajectory repetition rates for $\kappa_{\text{lin}} = 90$ % (4) and minimum step times (5)

Medium	Triangle f_∇ in Hz	Sawtooth $f_\vartriangle$ in Hz	Step time t_S in ms
Air	193.5	84.0	0.80
Silicone oil 1 cSt	82.0	35.6	1.90
Silicone oil 3 cSt	66.4	28.8	2.34
Ideally damped system design	114.0	49.5	1.36

5. DISCUSSION

After analyzing the different physical effects using silicone oil, the interest is in the total gain or loss in dynamic performance for future scanner designs including passive oil damping. While damping, permittivity and refractive index are rising with silicone oil, the system's eigenfrequency is decreasing and the maximum trajectory repetition rate respectively. To maintain the scanners total deflection and drive voltage of the system in silicone oil, the spring can be designed stiffer according the permittivity ε_r and refractive index n with:

$$k_{0,\text{oil}} = n \cdot \varepsilon_r \cdot k_{0,\text{air}}\,. \tag{6}$$

Nevertheless, the torque inertia increases due to moved silicone oil (cf. Tab. 2) compared to air by the relation:

$$J_{\text{rel}} := \frac{J_{\text{oil}}}{J_{\text{air}}}\,. \tag{7}$$

Considering (6) and (7) the equivalent total system's eigenfrequency $f_{0,\text{oil}}$ in oil becomes:

$$f_{0,\text{oil}} = \frac{1}{2\pi}\sqrt{\frac{k_{0,\text{oil}}}{J_{\text{oil}}}} = \frac{1}{2\pi}\underbrace{\sqrt{\frac{n\cdot\varepsilon_r}{J_{\text{rel}}}}}_{:=c_{\text{oil}}}\sqrt{\frac{k_{0,\text{air}}}{J_{\text{air}}}} = c_{\text{oil}} \cdot f_{0,\text{air}}\,. \tag{8}$$

According to (8) the equivalent system's eigenfrequency in oil towards air decreases by the factor c_{oil}. Consequently, the factor $c_{\text{oil}} := \sqrt{n \cdot \varepsilon_r / J_{\text{rel}}}$ describes the total loss in dynamic performance of trajectory and step according (4) and (5), which is comparable with a bandwidth reduction to 75 % for silicone oil 1 cSt and 61 % for silicone oil 3 cSt respectively.
The ideally damped system would have a quality factor of $Q = 1/\sqrt{2} = 0.7$, cf. Janschek (2012). By linear extrapolation of the quality factor the system parameters are approximated to a silicone oil viscosity of 3.43 cSt, a torque inertia of 4.55 kg µm² and a refractive index of $n = 1.4$. Consequently, this theoretically ideally damped system is stiffened by factor $n \cdot \varepsilon_r = 3.15$ and has an eigenfrequency of 330 Hz in oil,

Post-print version of the article: R. Schroedter, J. Grahmann, K. Janschek, "Silicone Oil Damping for Quasi-static Micro Scanners with Electrostatic Staggered Vertical Comb Drives", *8th IFAC Symposium on Mechatronic Systems*, vol. 52, issue 15, pp. 37-42, 2019. DOI: 10.1016/j.ifacol.2019.11.646

For further information contact: schroedter@acin.tuwien.ac.at, https://orcid.org/0000-0003-3259-4571

which is reduced by factor c_{oil} = 59 % compared to air. Then, the trajectory and step bandwidth, given in the last row in Tab. 3, are almost doubled compared to the experiments with silicone oil 3 cSt.

6. PACKAGING

The micro scanner must fully operate in silicone oil. Therefore, air bubbles, as shown in Fig. 7 (right), have to be avoided in the packaging. In a scan module the micro scanner is typically glued on electronics (PCB) and covered with glass for protection. The frame between PCB and glass cover serves as housing to create the cavity, that is filled with silicone oil, as shown in Fig. 12.

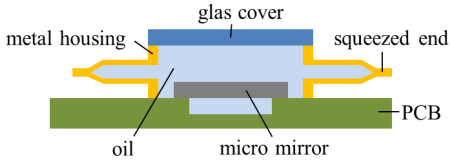

Fig. 12: Packaging variant without air bubbles

The proposed metal housing has an inflow (left) and an outflow (right) pipe for filling silicone oil into the cavity. Silicone oil fills easily between the 5 µm comb gaps due to capillary motion. Both pipes are squeezed after filling to close the cavity, which leads to a bubble-free packaging.

7. SUMMARY AND OUTLOOK

Quasi-static micro scanners operating in air have extremely low damping, which causes large parasitic oscillations while a trajectory is being tracked. Instead of applying complex and costly control strategies, this contribution investigates silicone oil as passive system damping for an electrostatic micro scanner with staggered vertical comb drives. On-chip piezoresistive feedback sensors serve for the experimentally system characterization in air and in silicone oil with 1 cSt and 3 cSt dynamic viscosity. Operating in silicone oil the system's damping as well as the permittivity and refractive index are increased, but the eigenfrequency decreases due to moved oil. The resulting mirror dynamics is verified by simulation and concluded with a factor describing the total dynamic system performance. Consequently, an equivalent micro scanner operating in silicone oil with a dynamic viscosity of 3.43 cSt would be optimally damped. When raising the spring stiffness by factor 3.15, the system's eigenfrequency indeed drops to 59 % compared to air, but no further control is required.

REFERENCES

Baumgart, M., Lenzhofer, M., Kremer, M. P., Tortschanoff, A. (2015). Integrated packaging of 2D MOEMS mirrors with optical position feedback. *Proc. SPIE 9375, MOEMS and Miniaturized Systems XIV*, 93750R, DOI: 10.1117/12.2079219

Chao, F., He, S., Chong, J., Mrad, B. R., Feng, L. (2011). Development of a micromirror based laser vector scanning automotive HUD. *IEEE Int. Conf. on Mechatronics and Automation*, Beijing, pp. 75-79, DOI: 10.1109/ICMA.2011.5985634

Grahmann, J., Dreyhaupt, A., Drabe, C., Schroedter, R., Kamenz, J., Sandner, T. (2016). MEMS-mirror based trajectory resolution and precision enabled by two different piezoresistive sensor technologies. *Proc. SPIE 9760, MOEMS and Miniaturized Systems XV*, 976006, DOI: 10.1117/12.2212965

Janschek, K. (2012). Mechatronic Systems Design - Methods, Models, Concepts. Springer. DOI: 10.1007/978-3-642-17531-2

Jiménez, A., Milde, T., Tatenguem, H., Honsberg, M., Carpintero, G., O'Gorman, J.; Sacher, J.R. (2018). MEMS-based widely tunable external cavity diode laser. *Proc. SPIE 10545, MOEMS and Miniaturized Systems XVII*, 105450J, DOI: 10.1117/12.2287849

Kaupmann, P., Pinter, S., Franz, J., Streiter, R., Otto, T. (2017). Design of a 2D MEMS micromirror with indirect static actuation. *IEEE SENSORS*, Glasgow, pp. 1-3, DOI: 10.1109/ICSENS.2017.8234252

Milanović, V., Kasturi, A., Yang, J. (2016). Novel fluidic packaging of gimbal-less MEMS mirrors for increased optical resolution and overall performance. *Proc. SPIE 9836, Micro- and Nanotechnology Sensors, Systems, and Applications VIII*, 98362Z, DOI: 10.1117/12.2224377

Milanović, V., Kasturi, A., Yang, J., Hu, F. (2017). Closed-loop control of gimbal-less MEMS mirrors for increased bandwidth in LiDAR applications. *Proc. SPIE 10191, Laser Radar Technology and Applications XXII*, 101910N, DOI: 10.1117/12.2264069

Park, Y., Moon, S., Lee, J., Kim, K., Lee, S.-J., Lee, J.-H. (2018). Gimbal-less two-axis electromagnetic microscanner with twist mechanism. *Micromachines*, vol. 9 (5), p. 219. DOI: 10.3390/mi9050219

Schroedter, R., Janschek, K., Sandner, T. (2014). Jerk and current limited flatness-based open loop control of foveation scanning electro-static micromirrors. IFAC Proceedings, vol. 47 (3), pp. 2685-2690. DOI: 10.3182/20140824-6-ZA-1003.02566

Schroedter, R., Roth, M., Janschek, K., Sandner, T. (2017). Flatness-based open-loop and closed-loop control for electrostatic quasi-static microscanners using jerk-limited trajectory design. *Mechatronics*, vol. 56, pp. 318-331, DOI: 10.1016/j.mechatronics.2017.03.005

Schroedter R. (2018). *Modellbasierter Systementwurf zur Steuerung und Regelung quasi-statischer Mikroscanner-spiegel mit elektrostatischem Kammantrieb*. Jörg Vogt Verlag, Dresden, Dissertation, 340 pages, ISBN: 9783959470308

Yalcinkaya, A. D., Urey, H., Brown, D., Montague, T., Sprague, R. (2006). Two-axis electromagnetic microscanner for high resolution displays. *Journal of Microelectromechanical Systems*, vol. 15 (4), pp. 786-794, DOI: 10.1109/JMEMS.2006.879380

Yoo, H. W., Druml, N., Brunner, D., Schwarzl, C., Thurner, T., Hennecke, M., Schitter, G. (2018). MEMS-based lidar for autonomous driving. *e & i Elektrotechnik und Informationstechnik*, vol. 135 (6), pp. 408–415, DOI: 10.1007/s00502-018-0635-2

Post-print version of the article: R. Schroedter, J. Grahmann, K. Janschek, "Silicone Oil Damping for Quasi-static Micro Scanners with Electrostatic Staggered Vertical Comb Drives", *8th IFAC Symposium on Mechatronic Systems*, vol. 52, issue 15, pp. 37-42, 2019. DOI: 10.1016/j.ifacol.2019.11.646

For further information contact: schroedter@acin.tuwien.ac.at, https://orcid.org/0000-0003-3259-4571